View metadata, citation and similar papers at core.ac.uk
brought to you by CORE
provided by CONICET Digital
Check for updates

Accepted Article

Article

Deactivation Study of Ru-Sn-B/Al_2O_3 Catalysts During Selective Hydrogenation of Methyl Oleate to Fatty Alcohol†

María A. Sánchez, María A. Vicerich, Vanina A. Mazzieri, Esteban Gioria
Laura B. Gutierrez, Carlos L. Pieck*

Instituto de Investigaciones en Catálisis y Petroquímica (INCAPE) (FIQ-UNL, CONICET), Colectora Ruta Nac. Nº 168 - Paraje El Pozo - CP 3000, Santa Fe, Argentina.

*Author to whom correspondence should be addressed: pieck@fiq.unl.edu.ar

†This article has been accepted for publication and undergone full peer review but has not been through the copyediting, typesetting, pagination and proofreading process, which may lead to differences between this version and the Version of Record. Please cite this article as doi: [10.1002/cjce.23444]

Received 6 August 2018; Revised 12 October 2018; Accepted 23 October 2018

The Canadian Journal of Chemical Engineering

This article is protected by copyright. All rights reserved

DOI 10.1002/cjce.23444

This article is protected by copyright. All rights reserved

Accepted Article

ABSTRACT

In this work the deactivation of the Ru-Sn-B/Al_2O_3 catalyst prepared by the incipient wetness method in the selective hydrogenation reaction of methyl oleate to fatty alcohol was studied. There was a decrease in both the activity and selectivity of fatty alcohol during successive reaction experiments. The fresh and deactivated catalysts were evaluated by different techniques such as TPR, XPS, TGA, Raman, and FTIR to determine the deactivation causes. Lower Ru and Sn content were found in the deactivated catalyst due to the loss of the active material during hydrogenation reaction. As the metal loss was more important for Ru than for Sn, the Ru/Sn ratio was changed, leading to a decrease of the selectivity. Moreover, the analysis of the XPS peak by the deconvolution of Sn species suggests the more active (SnO_x) species for selective hydrogenation are more affected than the less selective (SnO_y). Coke deposition was not observed by Raman and FTIR. This article is protected by copyright. All rights reserved

KEYWORDS: Ru-Sn-B/Al_2O_3 catalyst, deactivation, oleyl alcohol, selective hydrogenation

INTRODUCTION

Saturated and unsaturated fatty alcohols are used in the cosmetics industry as emollients, stabilizers, antifoaming agents, emulsifiers, and carriers. They are also used in other industries to produce surfactants and lube oils.[1] Fatty alcohol is commercially produced by selective hydrogenation at high pressure (20–35 MPa) using Cu-Cr or Zn-Cr catalysts from renewable sources (fatty acids, methyl esters, or wax esters).[2] Due to the commercial and environmental considerations, is important to achieve high activity and selectivity at lower pressures and/or lower H_2/oil ratios, since the major drawback is the high hydrogen compression costs. Moreover, for the high-pressure process, the capital costs are higher due to the cost of reactor construction material. Hydrogen storage and transportation and significant hydrogen consumption negatively impact the safety and efficiency of the hydrogenation process.[3] Another concern with these catalysts is the use, handling, and disposal of environmentally hazardous Cr compounds. Therefore, there is a considerable scientific research effort to replace this catalyst with a more selective and active one.[4] Noble metal supported catalysts were proposed, but these catalysts present higher activity with low selectivity. For this reason, some researchers are focused on catalysts with a noble metal and specific additives. The more commonly studied systems are Ru-Co[5,6] and Ru-Sn catalysts.[7,8]

The choice of an industrial catalyst should be based on its activity, selectivity, deactivation, regeneration, and cost. Deactivation of the catalysts is inevitable for a long or a short term and it can be the result of poisoning, fouling, thermal degradation, vapour formation, vapour-

This article is protected by copyright. All rights reserved

solid, and solid-solid reactions and attrition/crushing.[9] The deactivation causes of the catalysts must be known in order for them to be used for commercial purposes. Moreover, this knowledge will make it possible to change the reaction conditions or to improve the reagent purity.

It has been reported that the sulphur compounds present in the reactor feed deactivate the commercial Cu based catalysts used in the fatty esters hydrogenation.[10] Sulphur is known to strongly deactivate the metallic function of supported metal catalysts.[9] Usually, 1 Kg of copper catalyst per ppm of sulphur is required to produce 1 ton of fatty alcohols.[10] Other deactivation compounds of catalysts such as chlorine, nitrogen, and phosphorus compounds have been also found in natural fatty esters from coconut oil, palm oil, olive oil, sunflower oil, etc.[11]

As far as we are concerned, there are not any published works in the open literature about the deactivation of the Ru-Sn-B supported catalysts used for the selective hydrogenation of fatty esters or fatty acids. For this reason, the main objective of this work is to acquire information about the deactivation of Ru-Sn-B/Al_2O_3 catalysts used in the selective hydrogenation of methyl oleate to fatty alcohol.

Experimental Procedures

Catalyst preparation

The procedure to prepare the catalyst was previously reported.[12] In brief, the support γ-Al_2O_3 (Cyanamid Ketjen CK-300, pore volume = 0.5 cm^3g^{-1}, Sg (BET) = 180 m^2g^{-1}, 35–80 mesh) was impregnated with a $RuCl_3$ and $SnCl_2$ solution and reduced with sodium borohydride at room temperature (25 °C). Then, the catalyst was reduced in a hydrogen flow at 300 °C for 2 h.

Determination of the Ru, Sn, and B contents

The composition of the metallic phase was determined by inductively coupled plasma-optical emission spectroscopy (ICP-OES, Perkin Elmer, Optima 2100 DV) after acid digestion and dilution.

Temperature-programmed reduction (TPR)

The procedure was described previously.[12] It was carried out in a quartz reactor loaded with 200 mg of catalyst. The temperature was raised to 650 °C with a heating rate of 10 °C min^{-1}

This article is protected by copyright. All rights reserved

Accepted Article

using a mixture of H_2 (5 % v/v)-N_2 (9 cm^3 min^{-1}). Before the TPR experiment, the sample was heated in air flow at 450 °C for 1 h. The output of the reactor was connected to an on-line TCD to determine H_2 consumption.

X-ray photoelectron spectroscopy (XPS)

The XPS measurements were carried out using a SPECS multi-technique equipment with a dual Mg/Al X-ray source and a hemispherical PHOIBOS 150 analyzer operating in the fixed analyzer transmission (FAT) mode.[13] Previously, the samples had been reduced at 300 °C with H_2 (5 %)/Ar mixture for 10 min in a pre-treatment camera.

Thermogravimetric analysis (TGA)

A Mettler Toledo instrument with a TGA/SDTA851^e module was employed. 30–40 mg of sample placed inside a 70 μL alumina crucible was heated from 30–700 °C in a flow of nitrogen (50 cm^3min^{-1}). The heating rate of 10 °C min^{-1} was used. After the TGA experiments, the derivative thermogravimetric (DTG) profiles were calculated for the exact determination of the transition temperatures.

FTIR characterization

The FTIR spectra were recorded using a Shimadzu Prestige-21 spectrometer. For FTIR sample preparation, dried samples were blended with KBr (1:100) and pressed into wafers. The wafers were placed in the sample holder, and FTIR spectra were recorded in the range 4000–400 cm^{-1} in transmission mode with a spectral resolution of 4 cm^{-1}.

Laser Raman spectroscopy

The Raman spectra of the solids were recorded using a Horiba-Jobin-Yvon LabRam spectrometer with a 532 nm excitation wavelength. A 100X objective lens from an Olympus confocal microscope was used for simultaneous illumination and collection. The used spectrometer was equipped with a CCD detector that was cooled at ~203 K by Peltier effect. Each Raman spectrum was collected for 10 s and 10 accumulations with a laser power set at 30 mW.

Methyl oleate hydrogenation

The equipment and the reaction conditions were previously reported.[13] A stainless steel stirred autoclave (240 cm^3 effective volume) was used under the following operating

This article is protected by copyright. All rights reserved

Accepted Article

conditions: reaction time = 300 min; temperature = 290 °C; hydrogen pressure = 5 MPa; mass of catalyst = 1 g; methyl oleate mass = 3.5 g; solvent volume = 60 cm^3; and stirring speed = 800 rpm. Methyl oleate (99 %) and n-dodecane (99 %) were supplied by Sigma-Aldrich. In order to study the loss of activity and selectivity, several experiments were carried out using the same catalyst. The reaction mixture was discharged and filtered to retain the catalyst. The solid was conditioned by successive methanol washes at room temperature (25 °C), finally drying in an oven at 120 °C for 24 h. The established reaction parameters were the same as those used in previous work.[14]

RESULTS AND DISCUSSION

Figure 1 shows the conversion of methyl oleate as a function of the reaction time for four successive experiments. It can be observed that in the first ten minutes of the reaction all of the experiments show a high and almost similar increase in the conversion. After 10 min of reaction, the differences in catalyst activity become more evident. As evidenced by experiments 1–4, there was a significant decrease of the final conversion, falling from 98 to 60 %, which shows a marked reduction in catalyst activity. It is interesting to compare the deactivation of the Ru-Sn-B/Al_2O_3 catalyst with that of the commercial copper chromite. Rieke et al.[2] report that the Cu-Cr catalyst lost hydrogenation properties after five experiments of 10 h each at 280 °C and 13.8 MPa. The deactivation of commercial catalysts was also reported in the Thakur and Kundu's review.[15] They report that small amounts of free fatty acids, sulphur, chloride, water, phosphorous, glycerine, and monoglycerides present in the fatty acid methyl ester and wax ester feed may poison the catalyst and slow down the reaction rate. Voeste and Buchold[16] point out that the technical experience shows that 1 ppm sulphur above a certain level requires 1 kg additional catalyst per ton of fatty alcohol. The catalyst with 1000 ppm of S becomes nearly inactive. More experimental data on copper chromite deactivation were reported by Thakur et al.[17]

The results of selectivity to fatty alcohols, i.e., oleyl alcohol and stearyl alcohol, are shown in Figure 2. The total selectivity to fatty alcohols (stearyl and oleyl) always increases with reaction time, being ~ 95 % at the end of the run for the two first experiments. This fact shows the high selectivity of the catalyst. However, after each experiment the final selectivity decreases. In the second experiment, the total selectivity to fatty alcohols is smaller than the

This article is protected by copyright. All rights reserved

Accepted Article

total selectivity of the first experiment. In the third and fourth experiments, a strong reduction in the total selectivity to fatty alcohols is detected.

Oleyl alcohol is a reaction intermediate product of the methyl oleate hydrogenation, therefore, the selectivity passes through a maximum during the reaction time (Figure 3). Moreover, it is seen that the maximum is shifted to higher reaction times and the maximum value decreases after each experiment, indicating catalyst deactivation.

Table 1 shows the selectivity to all the reaction products observed at the maximum selectivity to oleyl alcohol. As shown in Figures 1–3, the conversion, as well as the selectivity to fatty alcohols, decreases with the number of experiments. The selectivity to oleyl alcohol is more affected than the selectivity to stearyl alcohol, while the selectivity to methyl stearate increases. These selectivity changes between different runs indicate that the deactivation affected the active sites of the catalysts differently in each test. The hydrogenation of the C = O group is catalyzed by Ru and SnOx in strong interaction, while the hydrogenation of the C = C double bond is only catalyzed by Ru atoms.

In previous works, we reported that the Ru with low or without interaction with the Sn only produces the hydrogenation of the double bond C = C, leading to the formation of methyl stearate.[18] Therefore, the loss of selectivity to fatty alcohols could be due to the segregation of the metals. However, other deactivation causes, such as coke deposition, sintering, or the elimination of metals during the reaction, or during the washing step of the catalyst before a new experiment, could not be ruled out. Poisoning by sulphur or other compounds is discarded because the reagents are pure.

In order to study the loss of the metal effect on the deactivation process during the washing step with methanol, a second hydrogenation reaction was performed using the unwashed catalyst. The selectivity and activity of the catalysts with and without washing were very similar (with variations between experimental errors, however, the results are not shown). This means that deactivation is not produced during the washing step.

This article is protected by copyright. All rights reserved

Accepted Article

Table 2 shows the values of metallic content of the fresh and used catalysts (four experiments) obtained by ICP-OES. A reduction in the amount of Ru (26 %) and Sn (21 %) is observed. The loss of the metal phase could occur mainly during the methyl oleate reaction because the activity and selectivity of the catalysts, washed and not washed with methanol, practically do not change. This hypothesis was confirmed by analyzing the reaction products with the same instrument. The results also showed the presence of Ru and Sn in the reaction medium.

Figure 4 shows the temperature-programmed reduction (TPR) profiles of the fresh and deactivated catalyst after four successive methyl oleate hydrogenation reactions. For the sake of simplicity, the TPR of monometallic catalysts were included although they were previously published.[18] The monometallic Sn catalyst is reduced between 150–500 °C. Two reduction zones are observed: one at 200–300 °C and the other one at 380–520 °C due to different interaction between the Sn oxides and the support.[18] Monometallic Ru/Al_2O_3 catalyst has two reduction peaks at 120 and 173 °C. The first peak was attributed to the reduction of the Ru chlorinated species and the second smaller peak to the reduction of the Ru oxide species.[19] It can be seen in Figure 4 that the Ru-Sn-B/Al_2O_3 fresh catalyst displays a large reduction peak centered at 200 °C due to the overlapping reduction of Ru oxides and the Sn species strongly interacting with Ru. There is also a reduction zone between 200–500 °C that could be assigned to the reduction of the Sn species segregated of the Ru. The catalyst used four times in the hydrogenation reactions (deactivated catalyst) displays a reduction profile similar to the fresh catalyst at a low temperature. However, the peak assigned to the segregated Sn species is not observed. After reaction, the hydrogen consumption decreases 26 % compared with the fresh solid. This result is in agreement with the metal phase loss values reported in Table 2. Consequently, a leaching effect during the reaction that leads to a partial removal of the Ru and Sn could be observed.

Chemical state of the metallic elements was determined by XPS. The peak of Ru $3d_{3/2}$ overlaps with the C 1s peak, and, thus, Ru $3d_{5/2}$ peak was used to analyze the chemical state of the Ru, while the Sn $3d_{5/2}$ was used to analyze the Sn species. Figure 5 shows the XPS spectra in the binding energy range of the Sn $3d_{5/2}$. Due to the proximity of the Sn^{2+} and Sn^{4+} peaks, the oxidation state of Sn cannot be determined. Nevertheless, Pouilloux et al.,[20] by

This article is protected by copyright. All rights reserved

Accepted Article

peak deconvolution, suggest the presence of SnO_x and SnO_y species, with $0 < x < y$. Moreover, these authors reported that the SnO_x species in interaction with ruthenium are the active sites for the selective hydrogenation reaction. Thus, it could be established that the lower selectivity to fatty alcohol observed in the used catalyst could be due to the lower amount of SnOx compared to the fresh one.

Table 3 reports the Ru/Al, Sn/Al, B/Al, Sn/Ru, and Cl/Al superficial atomic ratio obtained by XPS of the fresh and used catalysts. It could be concluded that the deactivated catalyst presents a decrease in the superficial content of Ru, Sn, Cl, and B. The Sn/Ru ratio of the used catalyst is higher than that of the fresh one. This is probably because more Ru was lost than Sn (Table 2). This not only modifies the amount of surface species but also their atomic ratio, leading to a loss of activity and selectivity. It was also reported that Sn/Ru = 2.0 is the optimal superficial ratio that favours the reaction of the hydrogenation of methyl oleate to oleyl alcohol.[21] Thus, the loss of active material has a harmful influence on selectivity and catalytic activity due to the modification of the superficial Ru/Sn ratio.

Figure 6 shows the FTIR spectra of the fresh and used catalysts with and without washing. All catalysts display the typical alumina absorption bands. The stronger broad band at ~3800–3000 cm^{-1} and the signal at the 1635–1350 cm^{-1} region correspond to bonded OH groups vibrations, while the bands at 755 and 590 cm^{-1} are assigned to the Al-O vibration of alumina.[22] The difference between the used/non-washed catalysts and the fresh catalyst together with the used/washed one is very clear. The unwashed catalyst presents the typical bands corresponding to different organic moieties: (i) 1200 and 1300 cm^{-1}; C-OH species (ii) 1300–1420 cm^{-1} symmetric COO stretching vibrations; (iii) ~1470 cm^{-1} C-H binding; (iv) 1540–1650 cm^{-1} asymmetric COO^- stretching frequencies; (v) 1690–1750 cm^{-1} C = O moieties in a carboxyl group, typically; and (vi) 2800–3000 cm^{-1} C-H bends. It should especially be observed the bands at ~2920 and 2852 cm^{-1} as they correspond to the symmetric stretching vibration of the CH_2 moieties. These bands suggest the presence of some waste solvent ($C_{12}H_{26}$).[23] Consequently, these results clearly show that, after reaction, in the non-washed catalyst some reagents and products remain adsorbed on the catalyst surface, possibly bound together by some coke. Then, it could be suggested that during the washing step almost all the reaction products are removed from the catalyst surface because the FTIR spectra is very similar to the fresh catalyst. These results lead to the conclusion that the washing effect improves the catalyst performance. However, coke formation during the reaction should not

This article is protected by copyright. All rights reserved

Accepted Article

be excluded. Coke is very difficult to eliminate by washing of the catalyst at room temperature (25 °C).

The Raman spectra were taken to evaluate the presence of coke. Signals at ~1339 (D mode) and 1593 (G mode) were attributed to carbonaceous species.[24] Therefore, the coke formation is excluded because these bands were not observed in both used washed and non-washed catalysts. Nevertheless, the non-washed deactivated solid presented typical bands of organic entities in the ranges of 1000–1600 and 2600–3000 cm^{-1} (Figure 7). In agreement with the FTIR results, the obtained Raman spectra clearly indicated that $C_{18}H_{38}O$, $C_{18}H_{36}O$, $C_{19}H_{36}OH$, $C_{18}H_{36}O_2$, $C_{12}H_{26}$, and their different isomers remained on the catalyst surface.[25]

The TGA experiments were performed in flowing nitrogen to confirm the presence of adsorbed species. Figure 8a shows the TGA profiles of the fresh catalyst and the used solids with and without washing. A 10 % total weight loss in the fresh catalyst and the washed one could be observed. The main drop of mass is between 30–120 °C, corresponding to the desorption of adsorbed water. On the other hand, for the non-washed used catalyst a 70% mass loss is observed. These results suggest the presence of several desorption processes of different organic compounds residuals from the reaction. The DTG result (Figure 8b) confirms that different desorption steps occur during the TGA experiment. The catalyst without washing showed three peaks at 240, 310, and 460 °C, confirming the presence of different products and reagent desorption processes.

A better analysis of the deactivation phenomena can be done by obtaining the pseudo first-order kinetic constants of the reactions and analyzing their variation upon deactivation. In a previous work a simple reaction model was formulated,[14] which was based on the reaction scheme proposed by Pouilloux et al.[26] The proposed model has only two rate constants: one for selective hydrogenation of carboxymethyl groups ($k_{C=O}$); and the other for C = C double bounds hydrogenation ($k_{C=C}$).[14]
The values of the kinetic constant have some uncertainty (from the statistical point of view) because the catalyst was deactivated during the reaction and the experimental points for each run are a few. The calculated kinetic constants are shown in Table 4.

This article is protected by copyright. All rights reserved

Accepted Article

It can be concluded that C = O hydrogenation is more affected by deactivation than C = C hydrogenation. Moreover, comparing the two first experiments the elimination of some Ru and Sn atoms first favours the hydrogenation of C = C double bonds. To explain this behaviour, it is necessary to consider that the hydrogenation of the C = C double bond is only catalyzed by Ru atoms.[20] The interaction of Ru with Sn decreases the hydrogenation activity of the C = C double bond.[12] Therefore, the elimination of some Sn produces Ru free atoms, which are active for the hydrogenation of the C = C double bond. On the other hand, the hydrogenation of the C = O group is catalyzed by Ru and Sn in strong interaction,[20] and , consequently the loss of one active site for C = O hydrogenation could be due to the loss of one Ru atom or one Sn atom.

CONCLUSIONS

The Ru-Sn-B/Al_2O_3 catalyst used in the selective hydrogenation of methyl oleate is deactivated during the reaction. The deactivation by coke deposition was discarded because typical spectroscopy peaks of coke were not observed by Raman.

The results of ICP/AES, XPS, and TPR show that there is a loss of Ru and Sn. As the metal loss was more important for Ru than for Sn, the Ru/Sn ratio was changed leading to a loss of the selectivity. Moreover, the analysis of the XPS peak by deconvolution of the Sn species suggests the more active (SnO_x) species for selective hydrogenation are more affected than the less selective (SnO_y).

REFERENCES

[1] K. Noweck, W. Grafahrend, *Ullmann's Encyclopedia of Industrial Chemistry,* Wiley-VCH, Weinheim **2006.**

[2] R. D. Rieke, D. S. Thakur, B. D. Roberts, G. T. White, *J. Am. Oil Chem. Soc.* **1997**, *74*, 341.

[3] Z. Zhang, F. Zhou, K. Chen, J. Fu, X. Lu, P. Ouyang, *Energ. Fuel.* **2017**, *31*, 12624.

[4] M. A. Sánchez, G. C. Torres, V. A. Mazzieri, C. L. Pieck, *J. Chem. Tech. Biot.* **2017**, *92*, 27.

[5] K. De Oliveira, Y. Pouilloux, J. Barrault, *J. Catal.* **2001**, *204*, 230.

[6] V. M. Deshpande, K. Ramnarayan, C. S. Narasimhan, *J. Catal.* **1990**, *121*, 174.

This article is protected by copyright. All rights reserved

Accepted Article

Accepted Article

[7] V. O. Rodina, D. Y. Ermakov, A. A. Saraev, S. I. Reshetnikov, V. A. Yakovlev, *Appl. Catal. B-Environ.* **2017**, *209*, 611.

[8] M. A. Sánchez, V. A. Mazzieri, M. A. Vicerich, C. R. Vera, C. L. Pieck, *Ind. Eng. Chem. Res.* **2015**, *54*, 6845.

[9] M. D. Argyle, C. H. Bartholomew, *Catalysts* **2015**, *5*, 145.

[10] D. S. Brands, G. U-A-Sai, E. K. Poels, A. Bliek, *J. Catal.* **1999**, *186*, 169.

[11] F. Th van de Scheur, G. U. Sai, A. Bliek, L. H. Staal, *J. Am. Oil Chem. Soc.* **1995**, *72*, 1027.

[12] M. A. Sánchez, Y. Pouilloux, V. A. Mazzieri, C. L. Pieck, *Appl. Catal. A-Gen.* **2013**, *467*, 552.

[13] M. A. Sánchez, V. A. Mazzieri, M. A. Vicerich, C. R. Vera, C. L. Pieck, *Ind. Eng. Chem. Res.* **2015**, DOI: http://dx.doi.org/10.1155/2015/561350.

[14] M. A. Sánchez, V. A. Mazzieri, M. R. Sad, C. L. Pieck, *React. Kinet. Mech. Cat.* **2012**, *107*, 127.

[15] D. S. Thakur, A. Kundu, *J. Am. Oil Chem. Soc.* **2016**, *93*, 1575.

[16] T. Voeste, H. Buchold, *J. Am. Oil Chem. Soc.* **1984**, *61*, 350.

[17] D. S. Thakur, B. D. Roberts, G. T. White, R. D. Rieke, *J. Am. Oil Chem. Soc.* **1999**, *76*, 995.

[18] M. A. Sánchez, V. A. Mazzieri, M. R. Sad, R. Grau, C. L. Pieck, *J. Chem. Technol. Biot.* **2011**, *86*, 447.

[19] V. A. Mazzieri, F. Coloma-Pascual, A. Arcoya, P. C. L'Argentière, N. S. Fıgoli, *Appl. Surf. Sci.* **2003**, *210*, 222.

[20] Y. Pouilloux, F. Autin, C. Guimon, J. Barrault, *J. Catal.* **1998**, *176*, 215.

[21] K. Y. Cheah, T. S. Tang, F. Mizukami, S. Niwa, M. Toba, Y. M. Choo, *J. Am. Oil Chem. Soc.* **1992**, *69*, 410.

[22] R. M. Mironenko, O. B. Belskaya, V. P. Talsi, T. I Gulyaeva, M. O. Kazakov, A. I. Nizovskii, V. A. Likholobov, *Appl. Catal. A-Gen.* **2014**, *469*, 472.

[23] H. Zhang, S. Shao, R. Xiao, D. Shen, J. Zeng, *Energ. Fuel.* **2014**, *28*, 52.

[24] B. Mutz, P. Sprenger, W. Wang, D. Wang, W. Kleist, J.-D. Grunwaldt, *Appl. Catal. A-Gen.* **2018**, *556*, 160.

[25] K. Tanabe, J. Hiraishi, *Spectral Database for Organic Compounds SDBS*, accessed on 20 April 2018, http://sdbs.db.aist.go.jp/sdbs/cgi-bin/cre_index.cgi.

[26] Y. Pouilloux, F. Autin, J. Barrault, *Catal. Today* **2000**, 63, 87.

This article is protected by copyright. All rights reserved

Figure Captions

Figure 1. Methyl oleate conversion as a function of the reaction time for the successive experiments.

Figure 2. Selectivity to fatty alcohol (oleyl alcohol + stearyl alcohol) as a function of reaction time for the successive experiments.

Figure 3. Selectivity to oleyl alcohol as a function of reaction time for the successive experiments.

Figure 4. TPR profiles of the fresh Ru/Al_2O_3, Sn/Al_2O_3, $Ru\text{-}Sn\text{-}B/Al_2O_3$, and used, washed $Ru\text{-}Sn\text{-}B/Al_2O_3$ four times catalysts.

Figure 5. XPS spectra of the Sn $3d_{5/2}$ of the used four times and fresh catalysts.

Figure 6. FTIR of the fresh and deactivated catalysts with and without washing.

Figure 7. Raman spectra of deactivated catalysts: A) non-washed; and B) washed.

Figure 8. Thermogravimetric measurements under nitrogen flow: a) TGA; and b) DTG (solid line: used non-washed catalyst; dot line: used washed catalyst; dash dot line: fresh catalyst).

Accepted Article

This article is protected by copyright. All rights reserved

Table 1. Conversion and selectivity to all reaction products in the maximum selectivity to oleyl alcohol observed in each experiment

Exp.	Reaction time (min)	Conversion (%)	Selectivity (%)		
			Oleyl alcohol	Stearyl alcohol	Methyl stearate
1	60	89.27	44.71	13.86	41.43
2	80	81.35	31.85	24.87	43.28
3	120	71.91	17.71	26.92	55.37
4	180	58.31	14.43	28.43	57.14

Accepted Article

This article is protected by copyright. All rights reserved

Table 2. Ru, Sn, and B contents on the fresh solids and on the used catalyst four times

Catalyst	Ru (wt%)	Sn (wt%)	B (wt%)
Fresh	0.92	1.90	0.38
Used	0.68	1.50	0.06

Accepted Article

This article is protected by copyright. All rights reserved

Table 3. Ru/Al, Sn/Al, Cl/Al, and B/Al atomic ratio obtained by XPS of fresh and used catalyst four times

Catalyst	Ru/Al	Sn/Al	$Ru^{\circ}/(Ru^{\circ}+Ru^{+})$	Sn/Ru	Cl/Al	B/Al
Fresh	0.010	0.020	0.27	1.941	0.025	0.012
Used	0.006	0.015	0.13	2.35	0.007	0.004

Accepted Article

This article is protected by copyright. All rights reserved

Table 4. Pseudo first-order kinetic constants as regressed from the experimental data

Test number	$K_{C=O}$ (s^{-1})	$K_{C=C}$(s^{-1})
1	1.49×10^{-4}	2.11×10^{-4}
2	1.17×10^{-4}	2.84×10^{-4}
3	5.02×10^{-5}	1.87×10^{-5}
4	3.32×10^{-5}	8.29×10^{-5}

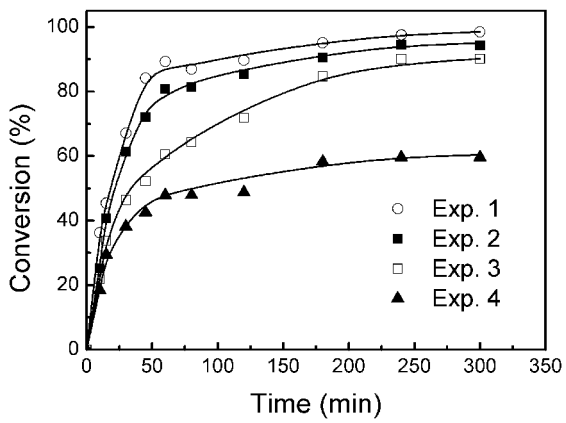

Figure 1

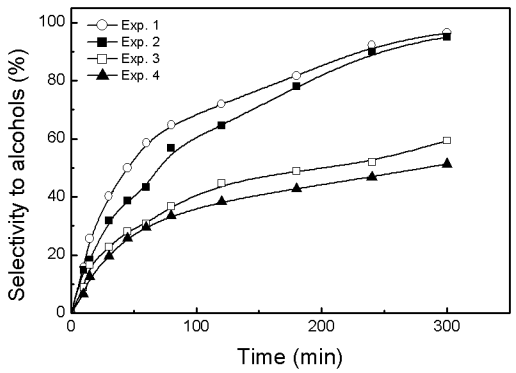

Figure 2

Accepted Article

This article is protected by copyright. All rights reserved

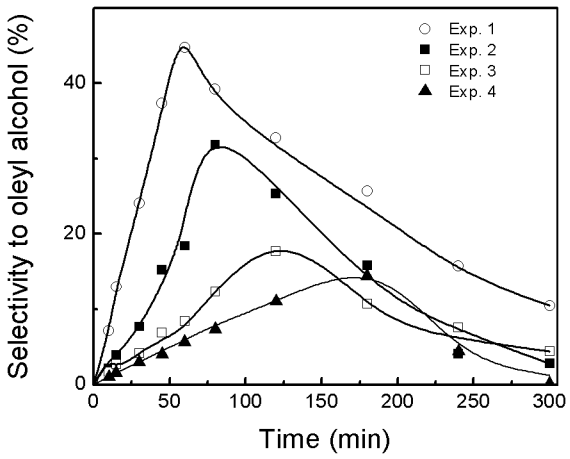

Figure 3

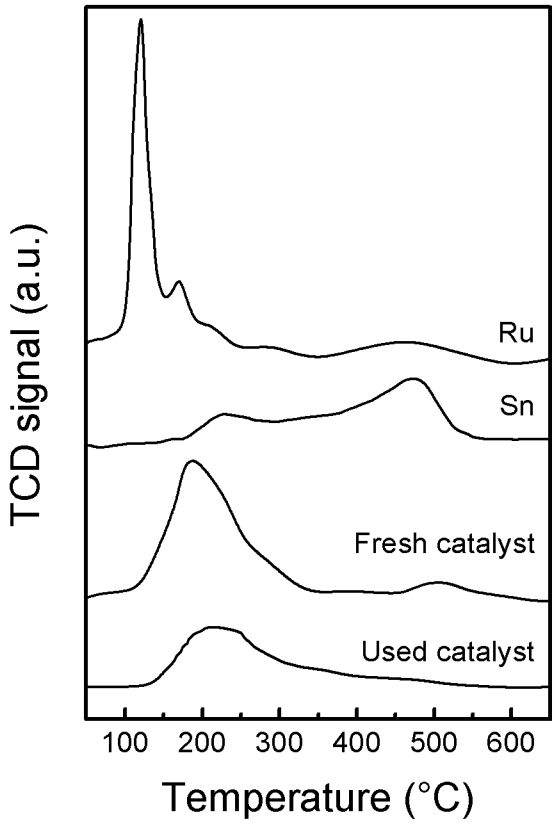

Figure 4

Accepted Article

This article is protected by copyright. All rights reserved

Accepted Article

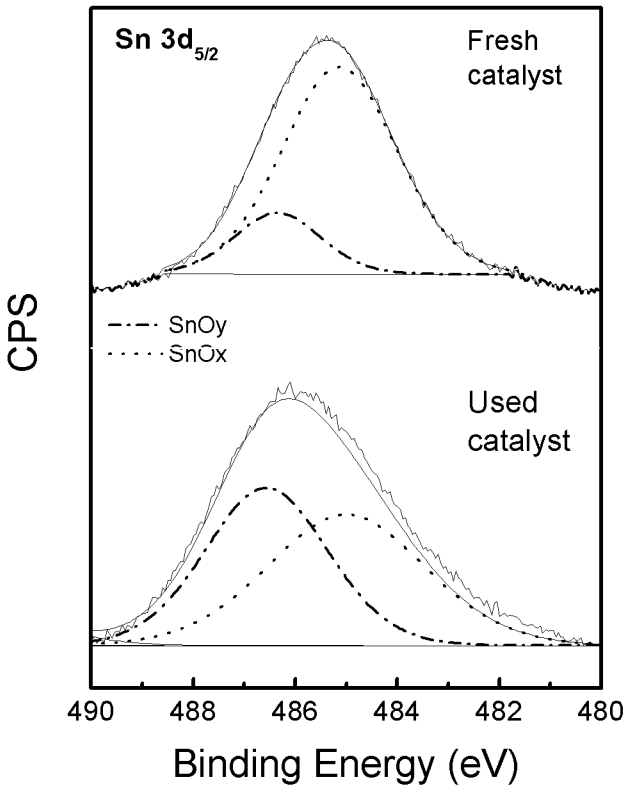

Figure 5

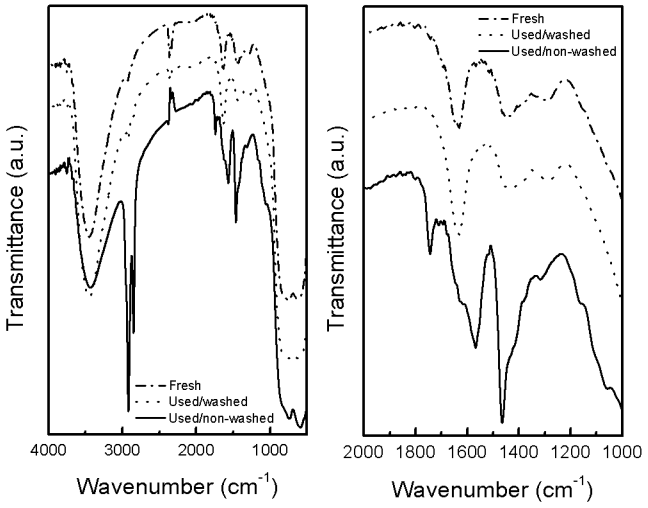

Figure 6

This article is protected by copyright. All rights reserved

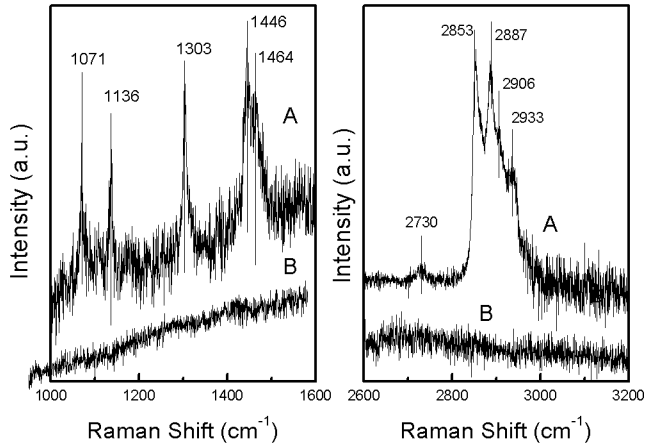

Figure 7

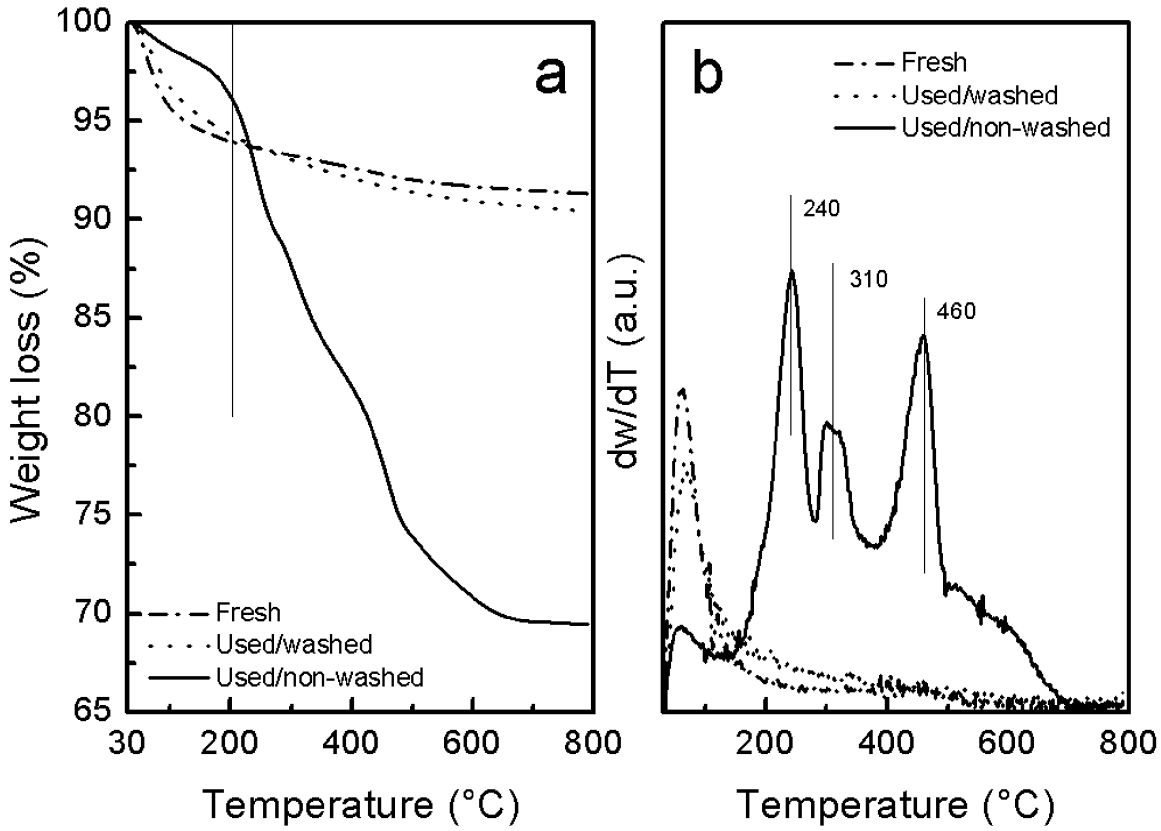

Figure 8

Accepted Article

This article is protected by copyright. All rights reserved